Front. Optoelectron. China 2008, 1(1–2): 101–108
DOI 10.1007/s12200-008-0014-4

RESEARCH ARTICLE

Investigation of spectral bandwidth of BBO-I phase matching non-collinear optical parametric amplification from visible to near-infrared

Bo LIU, Ruobing ZHANG (✉), Huagang LIU, Jing MA, Chen ZHU, Qingyue WANG

College of Precision Instrument and Opto-electronics Engineering, Key Laboratory of Optoelectronics Information and Technical Science, Tianjin University, Tianjin 300072, China

Abstract Laser sources which have high power, short time duration and are broadly tunable are needed for the application of ultra-fast lasers. Femtosecond optical parametric amplification (OPA) is one of the most important techniques to produce broadly tunable and several femtosecond laser pulses. To obtain an extremely short pulse, the femtosecond OPA should adequately support a large spectral bandwidth. Ultra-broadband type-I phase matching OPA based on BBO was theoretically investigated. The achromatic phase matching (APM) technology was introduced to femtosecond OPA, and a broadband phase matching condition was given when the signal beams were angularly dispersed. The methods were presented to choose the optimized non-collinear angle and angular dispersion. Effects of non-collinear angle and rate of angular dispersion to the parametric bandwidth were also discussed. The results indicate that a proper non-collinear angle of the non-collinear optical parametric amplifier (NOPA) and getting signal beams dispersed at the right rate in near-infrared conditions can increase the parametric bandwidth dramatically.

Keywords nonlinear optics, broadband femtosecond optical parametric amplification (OPA), angular dispersion, group velocity matching

1 Introduction

Femtosecond optical parametric amplification (OPA) is one of the important techniques for producing tunable ultra-short laser pulses due to its advantages of high gain in single pass and broad gain bandwidth. At present, the shortest pulse width from OPA is 4 fs [1], which was obtained from BBO-I phase matching OPA pumped by a light of 400 nm. To obtain shorter laser pulses from amplifiers, the OPA should support broader bandwidth. However, the bandwidth of OPA is limited by the phase matching condition. It was found that the gain bandwidth could increase by a non-collinear technique [2−9], and the broadband phase matching condition can be satisfied when the group velocities of the seed and the idle are matched [4,5]. However, in BBO type-I OPA pumped by light of 400 nm, group velocities matching (GVM) cannot be achieved when the seed wavelength is above 800 nm, so sub-10 fs pulses can only be obtained when the signal is visible.

In the 1990s, Martinez and Szabo proposed a technique of achromatic phase matching (APM) for the double-frequency process. In this APM scheme, broadband second-harmonic can be obtained by the introduction of spatial angular dispersion to make the different spectral components propagate at their phase matching angles [10,11]. In 2003 and 2004, sub-10fs ultraviolet (UV) pulses were obtained in an APM double-frequency process by using gratings and prisms to produce angular dispersion in the seed beams [12], and the APM technique was also used to improve bandwidth by a sum frequency mixing process to produce UV pulses [13].

In this paper, APM technology was introduced to improve the bandwidth of OPA. The NOPA of BBO type-I phase matching pumped by the blue light of 400 nm was theoretically investigated. A simple expression for broadband phase matching with angular dispersion of signal beams was given through a theoretical analysis of three pulses' phase mismatching. The methods were presented to choose the optimized non-collinear angle and angular dispersion for visible and near-infrared OPA. The effects of the non-collinear angle and angular dispersion of signal pulse on the parametric bandwidth

Translated from *Chinese Journal of Lasers*, 2007, 34(1): 19–26 [译自: 中国激光]

E-mail: zhangrb@tju.edu.cn

were also discussed. The results indicate that a suitable signal-pump angle and angular dispersion in a near-infrared signal pulse can increase the parametric bandwidth dramatically. The techniques and the analysis results provide a theoretical guidance for obtaining ultra-broadband parametric amplifiers.

2 Theoretical analyses

2.1 Broadband phase matching condition

In an OPA, three waves should satisfy the energy conservation law and the momentum conservation law as

$$\omega_p = \omega_s + \omega_i, \tag{1}$$

$$\boldsymbol{k}_p = \boldsymbol{k}_s + \boldsymbol{k}_i, \tag{2}$$

where the subscripts p, s and i denote pump, seed/signal and idle, respectively. ω refers to angular frequency and $\boldsymbol{k}$ is wave vector. The momentum conservation law is well known as a phase matching condition. Although this condition is not necessary, the phase mismatching will reduce the efficiency of OPA.

To determine the dependence of phase mismatch on angular frequency, the phase mismatch

$$\Delta\boldsymbol{k} = \boldsymbol{k}_p - \boldsymbol{k}_s - \boldsymbol{k}_i \tag{3}$$

can be expanded into a Taylor series as

$$\Delta\boldsymbol{k} = \Delta\boldsymbol{k}_0 + \frac{\partial\Delta\boldsymbol{k}}{\partial\omega_s}\Delta\omega_s + \frac{1}{2}\frac{\partial^2\Delta\boldsymbol{k}}{\partial\omega_s^2}(\Delta\omega_s)^2 + \cdots, \tag{4}$$

where $\Delta\boldsymbol{k}_0 = 0$, standing for ideal phase matching, is satisfied in the central frequency of the signal. If the first order

$$\frac{\partial\Delta\boldsymbol{k}}{\partial\omega_s} = 0, \tag{5}$$

the phase mismatch is determined by the second and higher order terms. Equation (5) is called the broadband phase matching condition of OPA.

In the non-collinear scheme, the relationship of three wave vectors is shown in Fig. 1. The vectorial phase mismatch $\Delta\boldsymbol{k}$ can be decomposed into the parallel and perpendicular components as

$$\Delta k_{//} = k_p - k_s\cos\alpha - k_i\cos\beta, \tag{6}$$

$$\Delta k_{\perp} = k_s\sin\alpha - k_i\sin\beta. \tag{7}$$

Assuming that $\Delta k_{\perp} = 0$, Eqs. (6) and (7) can be rewritten as

$$\Delta k = k_p - k_s\cos\alpha - k_i\cos\beta, \tag{8}$$

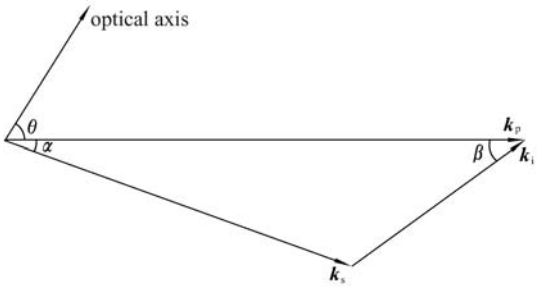

Fig. 1 Wave-vector geometry of type-I NOPA based on BBO

$$k_s\sin\alpha = k_i\sin\beta. \tag{9}$$

If seed beams are angularly dispersed, the differential of Eqs. (6) and (7) can be derived as

$$\frac{\partial\Delta k_{//}}{\partial\omega_s} = \frac{\partial k_s}{\partial\omega_s}\cos\alpha - k_s\frac{\partial\alpha}{\partial\omega_s}\sin\alpha + \frac{\partial k_i}{\partial\omega_s}\cos\beta - k_i\frac{\partial\beta}{\partial\omega_s}\sin\beta, \tag{10}$$

$$\frac{\partial\Delta k_{\perp}}{\partial\omega_s} = \frac{\partial k_s}{\partial\omega_s}\sin\alpha + k_s\frac{\partial\alpha}{\partial\omega_s}\cos\alpha - \frac{\partial k_i}{\partial\omega_s}\sin\beta - k_i\frac{\partial\beta}{\partial\omega_s}\cos\beta. \tag{11}$$

Multiplying Eq. (10) by $\cos\beta$ and Eq. (11) by $\sin\beta$ and adding the results, the following equation can be obtained:

$$\frac{\partial\Delta k_{//}}{\partial\omega_s}\cos\beta + \frac{\partial\Delta k_{\perp}}{\partial\omega_s}\sin\beta = -\frac{\partial k_s}{\partial\omega_s}\cos(\alpha+\beta) - \frac{\partial k_i}{\partial\omega_s} + k_s\frac{\partial\alpha}{\partial\omega_s}\sin(\alpha+\beta). \tag{12}$$

Assuming that the broadband phase matching condition Eq. (5) is fulfilled, $\frac{\partial\Delta k_{//}}{\partial\omega_s} = \frac{\partial\Delta k_{\perp}}{\partial\omega_s} = 0$. Equation (12) can be rewritten as

$$-\frac{\partial k_s}{\partial\omega_s}\cos(\alpha+\beta) - \frac{\partial k_i}{\partial\omega_s} + k_s\frac{\partial\alpha}{\partial\omega_s}\sin(\alpha+\beta) = 0. \tag{13}$$

If the pump is monochromatic, $\partial\omega_i = -\partial\omega_s$ and $\frac{\partial k_i}{\partial\omega_s} = \frac{\partial k_i}{\partial\omega_i}\frac{\partial\omega_i}{\partial\omega_s} = -\frac{\partial k_i}{\partial\omega_i}$. Equation (13) can be expressed as

$$k_s\frac{\partial\alpha}{\partial\omega_s}\sin(\alpha+\beta) + \frac{1}{v_i} - \frac{1}{v_s}\cos(\alpha+\beta) = 0, \tag{14}$$

where v_s and v_i are the group velocities of the signal and the idle respectively. Equation (14) is the broadband phase matching condition when angular dispersion is introduced to the signal beams. If the angular dispersion vanishes,

Eq. (14) can be simplified as

$$v_s = v_i \cos(\alpha + \beta). \tag{15}$$

Equation (15) shows that broadband phase matching can be achieved with a suitable signal-idler angle so that the signal group velocity is equal to the projection of the idler group velocity onto the signal wave vector [4,5]. Unfortunately, in some cases such as type-I phase matching OPA in BBO crystal pumped by a blue light of 400 nm, Eq. (15) cannot be satisfied by just changing the angle when the signal wavelength is above 800 nm. However, the introduction of angular dispersion in the signal can fulfill the broadband phase matching condition, as shown in Eq. (14).

2.2 Phase matching curves and broadband phase matching

In the BBO-I phase matching OPA, the pump is extraordinary light, while the seed and idle are ordinary (e→o+o). In the scheme of NOPA, according to Fig. 1, the following equation can be obtained:

$$k_i^2 = k_p^2 + k_s^2 - 2k_p k_s \cos\alpha. \tag{16}$$

Equation (16) can be written as

$$\frac{n_i^2}{\lambda_i^2} = \frac{n_p^2}{\lambda_p^2} + \frac{n_s^2}{\lambda_s^2} - \frac{2n_p n_s \cos\alpha}{\lambda_p \lambda_s}. \tag{17}$$

Together with Eqs. (1), (16) and (17), the solution of non-collinear angle α can be expressed as

$$\alpha = \arccos\left\{ \left(\frac{n_p^2}{\lambda_p^2} + \frac{n_s^2}{\lambda_s^2} - \frac{n_i^2}{\lambda_i^2} \right) \Big/ \left(\frac{2n_p n_s}{\lambda_p \lambda_s} \right) \right\}, \tag{18}$$

where $\frac{1}{n_p^2} = \frac{\cos^2\theta}{n_o^2(\lambda_p)} + \frac{\sin^2\theta}{n_e^2(\lambda_p)}$, and θ is the phase matching angle. n_o and n_e are the main axis refractive index, which can be given by the Sellmeier equation depending on the wavelength.

Figure 2 illustrates the dependence of non-collinear angle α on the signal wavelength in BBO type-I OPA pumped at 400 nm, with each curve representing a fixed phase matching angle. Figure 2 shows that when the phase-matching angle is at 0.55 rad, the phase matching curve is nearly a flat line from 550 to 700 nm, i.e., the non-collinear angle is approximately a constant with a value of 0.065 rad (3.7°). Choosing 0.55 and 0.065 rad as the phase matching angle and the non-collinear angle respectively, broadband phase matching and parametric gain can be achieved in the visible region. Moreover, the phase-matching curves above 800 nm have nearly direct lines of constant slope, the value of which is the angular dispersion. Thus, broadband phase matching in the near-infrared region can be achieved by introducing suitable angular dispersion in the signal beams.

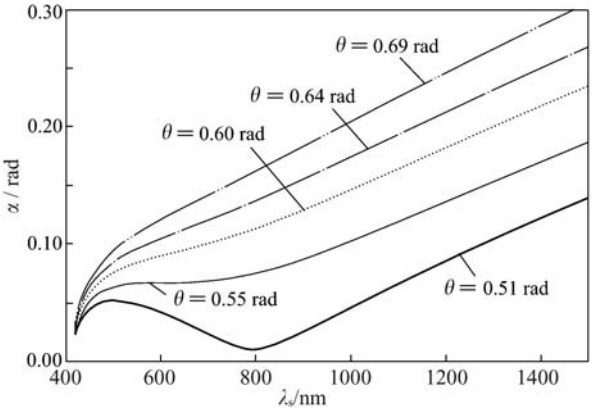

Fig. 2 Phase matching curves

To determine the angular dispersion of signal beams, Eq. (16) can be derived as

$$\frac{\partial\alpha}{\partial\lambda_s} = \left(k_i \frac{\partial k_i}{\partial\lambda_s} - k_s \frac{\partial k_s}{\partial\lambda_s} + k_p \frac{\partial k_p}{\partial\lambda_s}\cos\alpha \right) \Big/ \left(k_p k_s \sin\alpha \right). \tag{19}$$

With the aid of Eq. (1), $\frac{\partial k_i}{\partial\lambda_s} = \frac{\partial k_i}{\partial\omega_i}\frac{\partial\omega_i}{\partial\omega_s}\frac{\partial\omega_s}{\partial\lambda_s}$, $\frac{\partial k_s}{\partial\lambda_s} = \frac{\partial k_s}{\partial\omega_s}\frac{\partial\omega_s}{\partial\lambda_s}$, $\frac{\partial\omega_i}{\partial\omega_s} = -1$ and $\frac{\partial k}{\partial\omega} = v^{-1}$, Eq. (19) can be rewritten as

$$\frac{\partial\alpha}{\partial\lambda_s} = \frac{2\pi c}{\lambda_s^2} \frac{\frac{k_i}{v_i} + \frac{k_s}{v_s} - \frac{k_p\cos\alpha}{v_s}}{k_p k_s \sin\alpha}. \tag{20}$$

From Eq. (20) the proper angular dispersion of signal beams can be obtained.

3 Theoretical calculation of phase mismatch and parametric bandwidth

In the process of OPA, one criterion for the maximum allowable phase mismatching is given by [14] as

$$|\Delta \boldsymbol{k}| l_c = \pi, \tag{21}$$

where l_c is length of the nonlinear crystal. The conversion efficiency drops to approximately 0.4 when the phase mismatch is at the max value. Parametric bandwidth is defined as a signal spectral range in which normal phase mismatch $\Delta k l_c/\pi$ changes between -1 and $+1$. Parametric bandwidth, unlike gain bandwidth, is determined by phase mismatch and independent of the intensity of pump.

3.1 In the visible spectrum region

In BBO type-I phase matching OPA pumped by monochromatic light at 400 nm, if the seed wavelength is below 800 nm, broadband phase matching can be achieved by choosing the proper non-collinear angle α, which can be derived from Eqs. (2) and (15) as

$$\alpha = \arcsin\left[\frac{k_i}{k_p}\sqrt{1-\left(\frac{v_s}{v_i}\right)^2}\right]. \quad (22)$$

Figures 3 and 4 show the dependences of the signal-pump angle and the phase matching angle on the central wavelength of the seed below 800 nm. From Figs. 3 and 4, it is shown that if the seed wavelength is given, broadband phase matching can be obtained by choosing a proper signal-pump angle and a corresponding phase matching angle in the visible spectrum region. The solid line in Fig. 5 shows the dependence of parametric bandwidth on the central wavelength when the group velocities of the signal and idle are matched. In some references, the amount of $\Delta\boldsymbol{k}$ was calculated by expanding it into a Taylor series to second order [6,14]. In this paper, the amount of $\Delta\boldsymbol{k}$ is derived directly from Eq. (3). Figure 5 shows that parametric bandwidth larger than 160 nm can be obtained when the signal is tuned from 560 to 657 nm. As shown in Fig. 3, the corresponding signal-pump angle changes between 0.0641 rad (3.67°) and 0.0672 rad (3.85°), and the parametric bandwidth drops dramatically below the tuning range.

To explain this phenomenon, Fig. 6 illustrates the phase mismatch curves at 560 and 550 nm respectively. With reference to Fig. 6, the spectrum is divided into two parts at the signal wavelength of 550 nm (< 560 nm) in light of the phase mismatch tolerance criterion of Eq. (21), and the parametric bandwidth drops abruptly. In this case, if the signal-pump angle is slightly adjusted from 0.0625 rad (3.58°) to 0.065 rad (3.7°), the divided spectrum becomes continuous and parametric bandwidth can be improved from 81.9 to 213.5 nm as shown in Fig. 7. The situation is similar when the signal wavelength is above 657 nm.

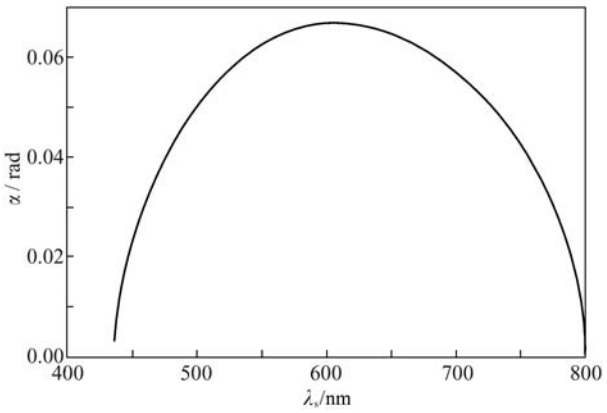

Fig. 3 Dependence of signal-pump angle on the signal wavelength when the velocities between signal and idle are matched

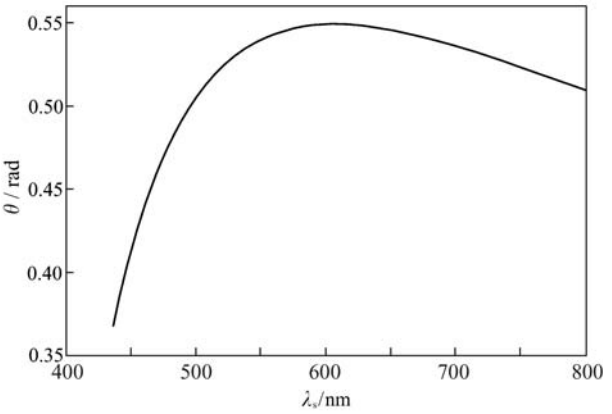

Fig. 4 Dependence of phase matching angle on the signal wavelength when the velocities between signal and idle are matched

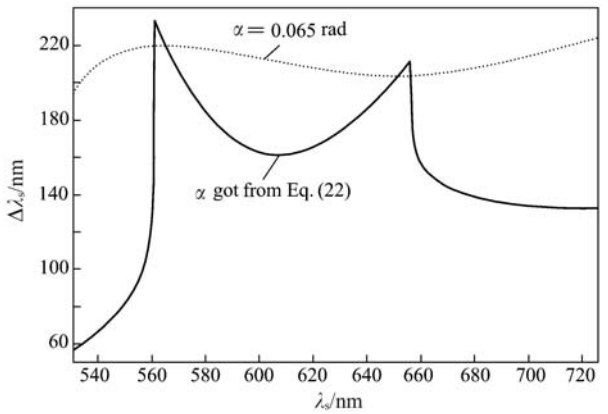

Fig. 5 Parametric bandwidth as a function of signal central wavelength in the visible spectrum

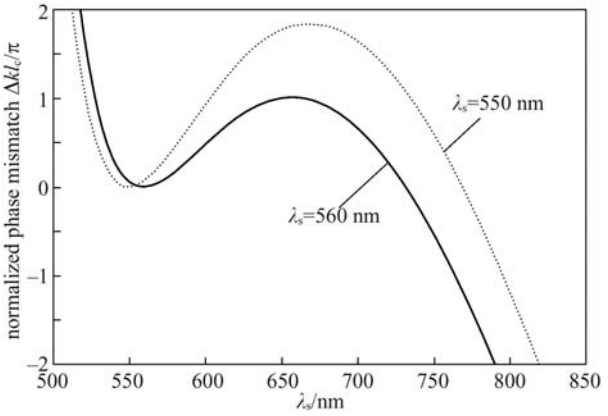

Fig. 6 Phase-mismatching curves at the central wavelength of 550 and 560 nm, respectively (group velocities of the signal and the idle are matched at the central wavelength)

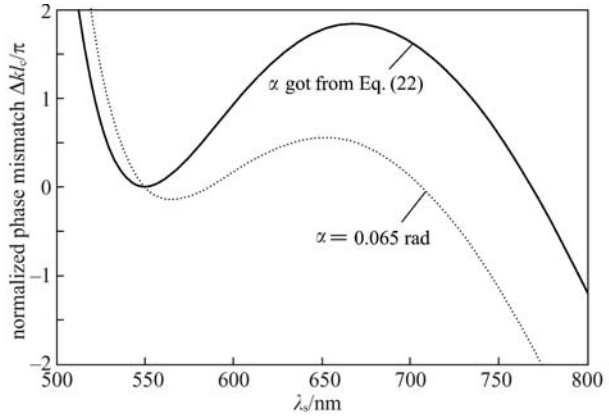

Fig. 7 Phase-mismatching curves with different signal-pump angles (central signal wavelength is 550 nm)

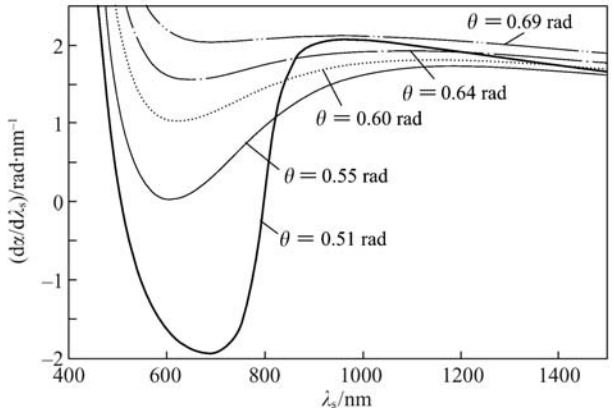

Fig. 8 Angular dispersion functions at central signal wavelength

The parametric bandwidth with a fixed signal-pump angle was also studied. The dotted line in Fig. 5 refers to the parametric bandwidth at a fixed non-collinear angle of 0.065 rad, where the length of the crystal is 1 mm. Figure 5 illustrates that at that angle, when the signal central wavelength is tuned from 531 to 726 nm, parametric bandwidths larger than 200 nm are available. From Fig. 2 it is shown that the tuning range just corresponds to the horizontal region of the phase matching curve at 0.55 rad. Based on experiments, 0.065 and 0.55 rad are thus the optimum choices for the non-collinear angle and phase matching angle.

3.2 In the near-infrared spectrum region

In the near-infrared spectrum region above 800 nm, the broadband phase matching condition of Eq. (5) can be achieved by introducing angular dispersion in the signal beams as shown in Eq. (14). Figure 2 shows that for the seed wavelength above 800 nm, the phase matching curves are nearly direct lines with constant slope. In this situation, broadband phase matching can be achieved when signal beams are angularly dispersed properly, and the signal-pump angle α and the rate of dispersion can be solved according to Eqs. (18) and (20). Figure 8 illustrates the dependence of rate of angular dispersion on the central wavelength of the signal. These curves are nearly horizontal in the near-infrared range above 800 nm, i.e., the rate of angular dispersion is approximately constant over a large range of the signal wavelength. When the signal is tuned to near-infrared, the rate of angular dispersion can be calculated from Eq. (20) to achieve broadband phase matching.

Figure 9 shows a comparison of the phase mismatch curve of angularly dispersed beams with collimate beams, when the central wavelength is 1000 nm and the phase matching angle is 0.64 rad. The solid line denotes the curve of phase mismatch for dispersed signal beams, and the rate of dispersion is 1.9182×10^{-4} rad/nm. There is no dispersion on the dotted line. As shown in Fig. 9, parametric bandwidth increases from 11 to 618 nm because of the dispersion of the signal beam, so signal beams with proper angular dispersion can improve the bandwidth dramatically.

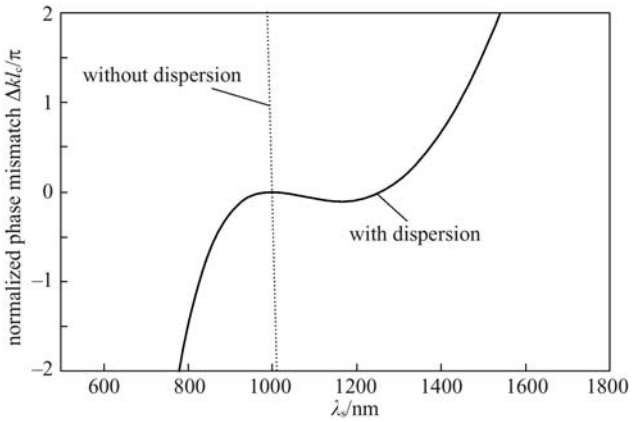

Fig. 9 Comparison of phase mismatch and parametric bandwidth whether seed beams are angularly dispersed or not

Figures 10(a) and 10(b) illustrate the curves of phase mismatch at different signal central wavelengths when the signal-pump angle α and the rate of angular dispersion are given by Eqs. (18) and (20), and phase matching angles are 0.64 and 0.69 rad respectively. According to Fig. 10, the curves of phase mismatch can be divided into four types in the region limited by the maximum phase mismatch tolerance of Eq. (21). Type-I has only one extreme value point (maximum or minimum) along the curve, such as the curves at central wavelength of 800 and 1400 nm in Fig. 10(a). Type-II curve has two extreme value points, such as the curve at wavelength of 1000 nm in Fig. 10(a). The parametric bandwidth of type-II is broader than that of type-I. Type-III curve has three extreme value points, including that at a wavelength of 1100 nm in Fig. 10(b). The

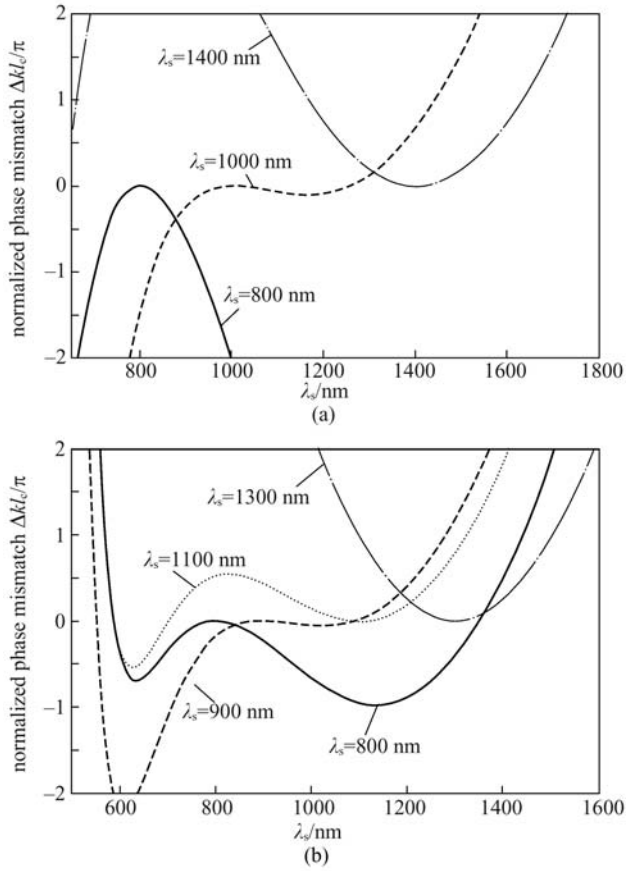

Fig. 10 Phase mismatching curves at different central wavelengths when the seed beams are angularly dispersed. (a) Phase matching angle is 0.64 rad; (b) phase matching angle is 0.69 rad

parametric bandwidth of this type is the largest. Type-IV is the monotonic curve without any extreme value point. The phase mismatch curve for collimate seed beams, such as the dotted line in Fig. 9, is the type-IV curve, and the bandwidth of this type is the narrowest. Figure 10(a) shows curves of phase mismatch at different signal central wavelengths of 800, 1000 and 1400 nm, with the phase matching angle at 0.64 rad. The calculations show that when the signal is tuned near 800 or 1500 nm, the phase mismatch curves are Type-I, as shown by the dotted-dash line and the solid line in Fig. 10(a). Tuning over the range of 920 to 1280 nm yields phase mismatch curves of type-II, such as the dashed line in Fig. 10(a) at the central wavelength of 1000 nm. For the phase match angle of 0.64 rad, parametric bandwidth in the middle of the near-infrared region is broader than that of the two sides. Similar results with Fig. 10(a) can be obtained when the phase matching angles are from 0.51 to 0.68 rad. Figure 10(b) shows the curves of phase mismatch at signal central wavelengths of 800, 900, 1100 and 1300 nm respectively, with the phase matching angle at 0.69 rad. When the signal is tuned over the range of 800 to 820 nm and of 1083 to 1132 nm, the phase mismatch curves are Type-III, as shown by the dotted line and the solid line in Fig. 10(b). For the range of 820 to 1083 nm the curves are type-II, such as the dashed line in Fig. 10(b), and in the range larger than 1132 nm the phase mismatch curves are type-I, as shown by the dotted-dashed line in Fig. 10(b). So for the phase match angle of 0.69 rad, parametric bandwidth in the short wavelength region of the near-infrared region is broader than that in the long wavelength region.

To compare the properties of parametric bandwidth for different phase matching angles, the dependence of parametric bandwidth on the central signal wavelength at phase matching angles 0.51, 0.60, 0.64 and 0.69 rad (Fig. 11) was investigated. It can be seen that in the middle part of the near-infrared region the parametric bandwidths are dramatically improved by the angularly dispersed seed beams. The bandwidths larger than 525, 595 and 560 nm can be achieved over the range of 877 to 1280 nm, 987 to 1360 nm and 920 to 1280 nm, respectively, and the corresponding phase matching angles are 0.51, 0.60 and 0.64 rad. However, in the spectrum region near 800 nm, the bandwidth obviously decreases. At the wavelength of 800 nm, the bandwidths are about 140, 180 and 230 nm, respectively. In the long wavelength region, the parametric bandwidth of 500, 510 and 455 nm can be obtained for phase matching angels of 0.51, 0.60 and 0.64 rad, which are slightly lower than that in the middle part of the near-infrared. It was also found that parametric bandwidth did not diminish near 800 nm at the phase matching angle of 0.69 rad, but started to decrease to 400 nm at central wavelength larger than 1130 nm. Considering both of the parametric bandwidths and large tuning range, 0.51 rad is the optimum phase matching angle. Parametric bandwidth larger than 500 nm is continuously available over the range from 877 to 1500 nm.

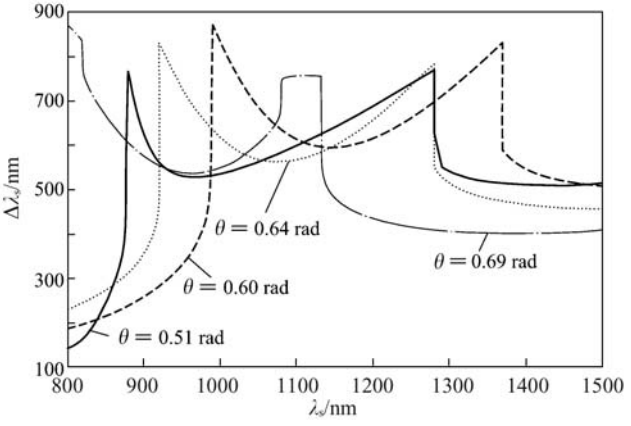

Fig. 11 Parametric bandwidth as a function of signal central wavelength in near-infrared spectral range with different phase matching angles, when the seed beams are angularly dispersed (ratio of dispersion are determined by Eq. (20); crystal length is 1 mm)

Taking the convenience of the experiments into account, the parametric bandwidth of OPA with a fixed rate of angular dispersion was also investigated over the whole tuning range. Firstly, a series of ratios of angular dispersion were calculated in the tuning range according to Eq. (20), with the median value chosen as the fixed rate. Tuning from 800 to 1500 nm, 1.893×10^{-4}, 1.762×10^{-4}, 1.885×10^{-4} and 2.073×10^{-4} rad/nm are selected as the ratios of angular dispersion for phase matching angles of 0.51, 0.60, 0.64 and 0.69 rad, respectively. The dependence of parametric bandwidth on the central signal wavelength is shown in Fig. 12. On the solid line, where the phase matching angle is 0.51 rad, the parametric bandwidth decreases to the range of 360 to 500 nm when the seed beams are tuned over the range of 828 to 958 nm; it decreases to the range of 230 to 300 nm near the central signal wavelength of 1500 nm. On the dotted-dashed line, where the phase matching angle is 0.69 rad, the bandwidth goes down to 480 nm over the range of 1030 to 1240 nm, and it also decreases dramatically over the range of 1360 to 1500 nm. Comparing Fig. 11 with Fig. 12, it can be seen that the parametric bandwidth in Fig. 12 is approximately equal to or wider than that in Fig. 11 except for the regions mentioned above. The calculation shows that decreases of bandwidth in these regions are due to division of the spectrum. This situation can be improved by choosing a different angular dispersion in a different section or changing the amount of angular dispersion slightly. In addition, at the phase matching angle of 0.60 rad, the bandwidth is larger than 780 nm over the range from 850 to 1500 nm as shown by the dashed line in Fig. 12. With the phase matching angle of 0.64 rad and corresponding rate of angular dispersion of 1.885×10^{-4} rad/nm, parametric bandwidth larger than 768 nm can be obtained in the range 800 to 1500 nm (the dotted line in Fig. 12), which is the optimum choice.

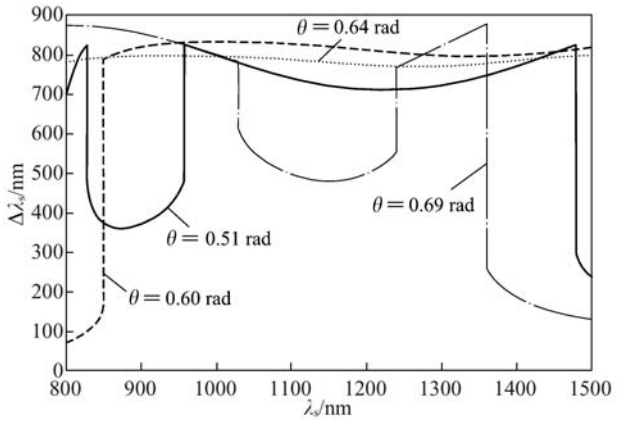

Fig. 12 Parametric bandwidth as a function of signal central wavelength in the near-infrared spectral range (the constant ratio of angular dispersion of seed beams are 1.893×10^{-4}, 1.762×10^{-4}, 1.885×10^{-4} and 2.073×10^{-4} rad/nm, corresponding to different phase matching angles of 0.51, 0.60, 0.64 and 0.69 rad; crystal length is 1 mm)

4 Conclusions

In this paper, BBO type-I phase matching femtosecond NOPA pumped by blue light of 400 nm was studied, and effects of the signal-pump angle and angular dispersion of signal beams on the phase mismatch and parametric bandwidth were theoretically calculated. In the visible range, the curves of signal-pump angle and phase matching angle as functions of the signal wavelength were given, when the group velocities of the signal and the idle were matched. It was also found that the parametric bandwidth and the tunable range can be promoted by adjusting the signal-pump angle, which makes group velocities between the signals and the idle mismatched slightly. The parametric bandwidth larger than 200 nm can be achieved at the tunable range from 531 to 726 nm, when the signal-pump angle is 0.065 rad and the phase matching angle is 0.55 rad. In the near-infrared, the results show that parametric bandwidth can be generally improved by introducing angular dispersion to the signal beams. The methods of determining phase matching angle, the non-collinear angle and rate of dispersion are given. Phase mismatch curves and parametric bandwidth were theoretically calculated on the conditions of satisfying broadband phase matching (Eq. (20)) and choosing fixed rate of angular dispersion. When the optimized parameters, the phase matching angle of 0.64 rad and the rate of angular dispersion of 1.885×10^{-4} rad/nm in the signal beams are selected, parametric bandwidth larger than 768 nm can be available at the tunable range from 800 to 1500 nm. These techniques presented to achieve broadband phase matching in this paper are quite universal and can be applied to different phase matching types, different nonlinear crystals and pump wavelength in principle. The optimized parameters can provide theoretical guidance for experiments to obtain broadband OPA.

Acknowledgements This research was supported by the National Key Basic Research Special Foundation of China (No. C1999075201) and the Specialized Research Fund for the Doctoral Program of Higher Education (No. 20030056021).

References

1. Baltuska A, Fuji T, Kobayashi T. Visible pulse compression to 4 fs by optical parametric amplification and programmable dispersion control. Optics Letters, 2002, 27(5): 306–308
2. Krylov V, Kalintsev A, Rebane A, et al. Noncollinear parametric generation in $LiIO_3$ and beta-barium borate by frequency-doubled femtosecond Ti:sapphire laser pulses. Optics Letters, 1995, 20(2): 151–153

3. Wilhelm T, Piel J, Riedle E. Sub-20-fs pulses tunable across the visible from a blue-pumped single-pass noncollinear parametric converter. Optics Letters, 1997, 22(19): 1494–1496
4. Shirakawa A, Kobayashi T. Noncollinear phase- and group-velocity matching of optical parametric amplifier for ultrashort pulse generation. IEICE Transactions on Electronics, 1998, E81C(2): 246–253
5. Riedle E, Beutter M, Lochbrunner S, et al. Generation of 10 to 50 fs pulses tunable through all of the visible and the NIR. Applied Physics B, 2000, 71(3): 457–465
6. Liu H J, Zhao W, Chen G F, et al. Investigation of spectral bandwidth of optical parametric amplification. Applied Physics B, 2004, 79(5): 569–576
7. Leng Y X, Jin S Q, Peng J H, et al. Investigation of noncollinear type-I phase matched optic parametric amplification using BBO crystal. Chinese Journal of Lasers, 2001, A28(11): 977–980 (in Chinese)
8. Liu H J, Chen G F, Zhao W, et al. Study on the bandwidth of three-wave mixing optical parametric amplifiers. Chinese Journal of Lasers, 2002, A29(8): 680–686 (in Chinese)
9. Yang X D, Xu Z Z, Zhang Z Q, et al. Experimental study on the gain bandwidth of non-collinear type-I optic parametric chirped pulse amplification using BBO crystal. Acta Optica Sinca, 2000, 20(8): 1151–1152 (in Chinese)
10. Szabo G, Bor Z. Broadband frequency doubler for femtosecond pulses. Applied Physics B, 1990, 50(1): 51–54
11. Martinez O E. Achromatic phase matching for second harmonic generation of femtosecond pulses. IEEE Journal of Quantum Electronics, 1989, 25(12): 2464–2468
12. Baum P, Lochbrunner S, Riedle E. Tunable sub-10-fs ultraviolet pulses generated by achromatic frequency doubling. Optics Letters, 2004, 29(14): 1686–1688
13. Nabekawa Y, Midorikawa K. Group-delay-dispersion-matched sum-frequency mixing for the indirect phase control of deep ultraviolet pulses in the sub-20-fs regime. Applied Physics B, 2004, 78(5): 569–581
14. Barnes N P, Corcoran V J. Parametric generation processes: spectral bandwidth and acceptance angles. Applied Optics, 1976, 15(3): 696–699